

## HARMONIC VIBRATION AND RESONANCE EFFECTS IN THE CASE OF LONGITUDINAL SHEAR OF A HOLLOW CYLINDER WITH CRACK

O. I. Kyrylova<sup>1,3</sup> and V. V. Mykhas'kiv<sup>1,2</sup>

UDC 539.3

We propose an efficient analytic-numerical method for the evaluation of dynamic stresses in a hollow cylindrical body of arbitrary cross section with a through crack under the conditions of antiplane deformation. This method enables us to separately solve the integral equations on the surface of the defect and satisfy the conditions of harmonic loading on the boundary of the body. We deduce the formulas for the dynamic stress intensity factors in the vicinity of the crack and study the influence of its geometric parameters and the frequency of vibration on the indicated factors, in particular, with the evaluation of resonance frequencies.

**Keyword:** hollow cylinder, tunnel crack, harmonic load, stress intensity factor, resonance effects, method of integral equations.

### Introduction

The analysis of the stressed state of bounded bodies with cracks under harmonic loads is quite urgent both for the diagnostics of defects, in view of the information about their influence on the resonance frequencies of vibration [1], and for the determination of the conditions of fracture of the bodies by estimating the stress intensity factors in the vicinity of the cracks [2]. The preliminary results in this direction were mainly obtained for bounded and semibounded bodies with cracks or thin inclusions [3–12]. The situations in which the bodies occupy bounded domains were studied less comprehensively. This is explained by the fact that, by applying the method of boundary integral equations, the original problems are reduced to connected systems of integral equations given both on the surfaces of defects and on the boundary of the body [13–17]. This explains the observed significant complication of the numerical realization of the method, especially for multiply connected domains. In what follows, we propose an approach that makes it possible to solve the integral equations on the surfaces of cracks and satisfy the conditions of loading on the boundary of the body.

### Formulation of the Problem

Consider an infinite hollow elastic cylinder with elements parallel to the  $Oz$ -axis (Fig. 1). The section of this cylinder by the plane  $xOy$  is a doubly connected domain bounded by arbitrary closed smooth curves. In a polar coordinate system  $Or\varphi$ , these curves are described by the following equations:  $r_0 = r_0\psi_0(\varphi)$  for the outer boundary of the cross section and  $r_1 = r_1\psi_1(\varphi)$  for its inner boundary;  $0 \leq \varphi < 2\pi$ .

<sup>1</sup> Pidstryhach Institute for Applied Problems in Mechanics and Mathematics, Ukrainian National Academy of Sciences, Lviv, Ukraine.

<sup>2</sup> Corresponding author; e-mail: tex@iapmm.lviv.ua.

<sup>3</sup> “Odesa Maritime Academy” National University, Odesa, Ukraine.

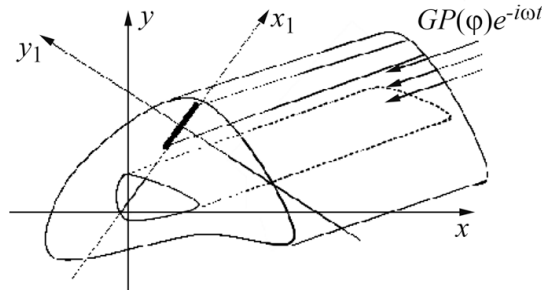


**Fig. 1.** Hollow cylinder with through crack.

The cylinder contains a through crack, which occupies a segment of length  $2a$  in the plane  $xOy$  and does not go beyond the boundaries of the cross section.

The process of longitudinal shear vibration in the body is caused by the action of a load  $P(\varphi)e^{-i\omega t}$  harmonic in time  $t$  and directed along the  $Oz$ -axis on the lateral surface of the cylinder, where  $P(\varphi)$  is a given amplitude of load and  $\omega$  is its circular frequency.

In what follows, the factor  $e^{-i\omega t}$  is omitted in our analysis. Under the formulated conditions, the cylinder is in the state of antiplane deformation in which solely the  $z$ -component of the vector of displacements  $w$  is not equal to zero. This component satisfies the Helmholtz equation [18], which takes the following form in the polar coordinate system:

$$\Delta w + \kappa_2^2 w = 0, \quad (1)$$

$$\Delta = \frac{\partial^2}{\partial r^2} + \frac{1}{r} \frac{\partial}{\partial r} + \frac{1}{r^2} \frac{\partial^2}{\partial \varphi^2},$$

where

$$\kappa_2^2 = \omega^2 c_2^{-2}, \quad c_2^2 = G\rho^{-1},$$

and  $G$ , and  $\rho$  are the shear modulus and the density of the material of the cylinder, respectively.

We describe the load on the outer boundary of the cylindrical body by the following boundary conditions for the tangential stresses  $\tau_{nz}$ :

$$\tau_{nz}(r_0 \psi_0(\varphi), \varphi) = GP(\varphi), \quad 0 \leq \varphi < 2\pi, \quad (2)$$

where  $\bar{n}$  is the vector of normal to the surface.

Assume that the inner boundary of the body is immobile. Then

$$w(r_1 \psi_1(\varphi), \varphi) = 0, \quad 0 \leq \varphi < 2\pi. \quad (3)$$

For the formulation of the boundary conditions on the crack, we choose a local coordinate system  $O_1 x_1 y_1$  such that the defect is located in the plane  $y_1 = 0$  (Fig. 1). The surface of the crack is assumed to be free of loads. Then

$$\tau_{zy_1}(x_1, 0) = 0, \quad |x_1| < a. \quad (4)$$

Let  $w^{(1)}(x_1, y_1)$  be the  $z$ -component of the vector of displacements  $w$  in the case of transition from the polar coordinate system to the Cartesian coordinates  $O_1x_1y_1$ . On the crack surface, the displacement  $w^{(1)}(x_1, y_1)$  is discontinuous with a jump described by the function

$$\chi(x_1) = w^{(1)}(x_1, +0) - w^{(1)}(x_1, -0), \quad \chi(\pm a) = 0. \quad (5)$$

Thus, we reduce the analysis of the steady (in time) deformation of the analyzed body weakened by a crack to the solution of the differential equation (2) with the boundary conditions (2)–(5).

### Scheme of Satisfying the Boundary Conditions on the Crack

We first consider a discontinuous solution  $w_1^{(1)}$  of the Helmholtz equation (1) with jump (5) on the crack surface, which takes the following form in the coordinate system  $x_1O_1y_1$  [3, 12]:

$$w_1^{(1)}(x_1, y_1) = \frac{\partial}{\partial y_1} \int_{-a}^a \chi(\eta) f(\eta - x_1, y_1) d\eta, \quad (6)$$

$$f(\eta - x_1, y_1) = -\frac{i}{4} H_0^{(1)} \left( \kappa_2 \sqrt{(\eta - x_1)^2 + y_1^2} \right).$$

In relation (6),  $H_0^{(1)}$  is the Hankel function of the first kind of order zero.

Further, in the polar coordinate system  $O_r\varphi$ , we represent the displacements in the cylinder in the form of superposition of two components, namely,

$$w(r, \varphi) = w_0(r, \varphi) + w_1(r, \varphi), \quad (7)$$

where  $w_1(r, \varphi)$  is displacement (6) after transition to the polar coordinates and  $w_0(r, \varphi)$  is the solution of the Helmholtz equation (1), which is later used to satisfy the boundary conditions (2) and (3).

We seek this solution in the form of a linear combination of  $N$  partial solutions of the Helmholtz equation (1), which are linearly independent in the cross-sectional region and form a complete closed system of functions [19]:

$$w_0(r, \varphi) = r_0 \sum_{k=1}^N (A_k g_k(r, \varphi) + B_k h_k(r, \varphi)), \quad (8)$$

$$g_{2m-1}(r, \varphi) = J_{m-1}(\kappa_2 r) \cos(m-1)\varphi, \quad g_{2m}(r, \varphi) = J_m(\kappa_2 r) \sin m\varphi,$$

$$h_{2m-1}(r, \varphi) = H_{m-1}^{(1)}(\kappa_2 r) \cos(m-1)\varphi, \quad h_{2m}(r, \varphi) = H_m^{(1)}(\kappa_2 r) \sin m\varphi.$$

In relations (8),  $A_k$  and  $B_k$  are unknown coefficients and  $J_m$  and  $H_m^{(1)}$  are cylindrical functions.

To satisfy the boundary conditions on crack (4), we pass to the coordinate system  $O_1x_1y_1$  in representation (7). This yields

$$w^{(1)}(x_1, y_1) = w_0^{(1)}(x_1, y_1) + w_1^{(1)}(x_1, y_1), \quad (9)$$

$$w_0^{(1)}(x_1, y_1) = r_0 \sum_{k=1}^N \left[ A_k g_k^{(1)}(x_1, y_1) + B_k h_k^{(1)}(x_1, y_1) \right].$$

Further, we substitute relation (9) in the boundary condition (4) and arrive at the integral equation for the derivative of the jump of displacements on the crack  $\chi'$ . We separate the singular part of this equation and use the following notation:

$$\eta = a\tau, \quad x_1 = a\zeta, \quad \kappa_0 = \kappa_2 r_0, \quad \frac{a}{r_0} = \gamma, \quad \kappa_2 a = \gamma \kappa_0, \quad \frac{r_1}{r_0} = \lambda.$$

As a result, the equation takes the form

$$\frac{1}{2\pi} \int_{-1}^1 \chi'(a\tau) \left[ \frac{1}{\tau - \zeta} + Q(\tau - \zeta) \right] d\tau = f(\zeta), \quad (10)$$

where  $Q$  is the regular component of the kernel (here, we do not present the expression for this component because it is too cumbersome) and

$$f(\zeta) = \sum_{k=1}^N \left( A_k f_k^1(\zeta) + B_k f_k^2(\zeta) \right),$$

$$f_k^1(\zeta) = -\frac{\partial g_k^{(1)}(a\zeta, 0)}{\partial y_1}, \quad f_k^2(\zeta) = -\frac{\partial h_k^{(1)}(a\zeta, 0)}{\partial y_1}.$$

In view of linearity, the solution of the integral equation (10) can be represented via the new unknown functions  $S_k^j$  ( $j = 1, 2$ ) as follows:

$$\chi'(a\tau) = \sum_{k=1}^N \left( A_k S_k^1(\tau) + B_k S_k^2(\tau) \right). \quad (11)$$

As a result, this equation turns into a sequence of equations for the functions  $S_k^j$  ( $j = 1, 2$ ), which differ only by right-hand sides, namely,

$$\frac{1}{2\pi} \int_{-1}^1 S_k^i(\tau) \left[ \frac{1}{\tau - \zeta} + Q(\tau - \zeta) \right] d\tau = f_k^i(\zeta), \quad i = 1, 2, \quad k = \overline{1, N}. \quad (12)$$

Equations (12) should be supplemented by the equalities, which follow from the conditions of crack closure at the crack tips:

$$\int_{-1}^1 S_k^i(\tau) d\tau = 0. \quad (13)$$

To construct approximate solutions of the system of equations (12), (13), we separate the square-root factor in the form

$$S_k^i(\tau) = \frac{\Psi_k^i(\tau)}{\sqrt{1-\tau^2}}. \quad (14)$$

Further, by using the method of mechanical quadratures [20, 21] in which the roots of the Chebyshev polynomial  $U_{n-1}(\zeta)$ ,

$$\zeta_j = \cos \frac{\pi j}{n}, \quad j = 1, 2, \dots, n-1,$$

play the role of collocation points, from the integral equations (12) and (13), we obtain the following system of linear algebraic equations for the values  $\Psi_{km}^i$  of the functions  $\Psi_k^i(\tau)$  at the interpolation nodes:

$$\begin{aligned} \frac{1}{2\pi} \sum_{m=1}^n a_m \Psi_{km}^i \left[ \frac{1}{\tau_m - \zeta_j} + Q(\tau_m - \zeta_j) \right] &= f_k^i(\zeta_j), \quad i = 1, 2, \quad k = \overline{1, n-1}, \\ \frac{1}{2\pi} \sum_{m=1}^n a_m \Psi_{km}^i &= 0. \end{aligned} \quad (15)$$

Solving Eqs. (15), we approximately restore each function  $\Psi_k^i(\tau)$  by the interpolation polynomial

$$\Psi_k^i(\tau) \approx \sum_{m=1}^n \Psi_{km}^i \frac{T_n(\tau)}{(\tau - \tau_m) T_n'(\tau_m)}, \quad (16)$$

where

$$\Psi_{km} = \Psi_k(\tau_m) \quad \text{and} \quad \tau_m = \cos \frac{\pi(2m-1)}{2n}, \quad m = 1, \dots, n,$$

are the roots of the Chebyshev polynomial of the first kind  $T_n(\tau)$ .

### Scheme of Satisfying of the Boundary Conditions on the Lateral Surfaces of the Cylinder

We now determine the unknown coefficients  $A_k$  and  $B_k$  appearing in representation (8) from conditions (2) and (3) on the surfaces of the cylinder. For this purpose, from relations (7), we find the boundary values of displacements and the corresponding stresses:

$$\tau_{\bar{n}z}(r_0\Psi(\varphi), \varphi) = \tau_{xz}(r_0\Psi(\varphi), \varphi) c_x + \tau_{yz}(r_0\Psi(\varphi), \varphi) c_y, \quad (17)$$

where  $c_x$  and  $c_y$  are the components of the normal  $\bar{n}$  to the outer boundary of the cross section.

Substituting the boundary values of displacements and stresses in conditions (2) and (3), we arrive at the following relations:

$$\begin{aligned} \sum_{k=1}^N A_k \left( \int_{-1}^1 \Phi_k^1(\tau) G(\tau, \varphi) d\tau + F_k^1(\varphi) \right) + \sum_{k=1}^N B_k \left( \int_{-1}^1 \Phi_k^2(\tau) G(\tau, \varphi) d\tau + F_k^2(\varphi) \right) &= P(\varphi), \\ \sum_{k=1}^N A_k \int_{-1}^1 \Phi_k^1(\tau) E(\tau, \varphi) d\tau + \sum_{k=1}^N B_k \int_{-1}^1 \Phi_k^2(\tau) E(\tau, \varphi) d\tau & \\ = - \left( \sum_{k=1}^N A_k g_k(r_1(\varphi), \varphi) + \sum_{k=1}^N B_k h_k(r_1(\varphi), \varphi) \right). & \end{aligned} \quad (18)$$

Here, the functions  $G(\tau, \varphi)$  and  $E(\tau, \varphi)$  are the combinations of the function  $f(\eta - x_1, y_1)$  from Eq. (6) and its derivatives on the outer boundary of the cross section and we represent  $F_k^1(\varphi)$  and  $F_k^2(\varphi)$  via the values of the derivatives of the functions  $g_k(r, \varphi)$  and  $h_k(r, \varphi)$  from Eq. (8) on this boundary. In deducing relations (18), we also used the equality

$$\chi(a\tau) = a \sum_{k=1}^N \left( A_k \Phi_k^1(\tau) + B_k \Phi_k^2(\tau) \right), \quad \left( \Phi_k^i(\tau) \right)' = S_k^i(\tau), \quad i = 1, 2,$$

which follows from representation (11).

To compute the integrals in equalities (18), it is necessary to use the following approximation [12] for the functions  $\Phi_k^i(\tau)$  obtained from relations (14) and (16):

$$\begin{aligned} \Phi_k^i(\tau) &\approx \sqrt{1 - \tau^2} S_{kn}^i(\tau), \\ S_{kn}^i(\tau) &= -\frac{2}{n} \sum_{m=1}^n \psi_{km}^i \sum_{p=1}^{n-1} \frac{T_p(\tau_m) U_{p-1}(\tau)}{p}, \end{aligned}$$

where  $U_{p-1}(\tau)$  is a Chebyshev polynomial of the second kind. As a result, we compute the integrals in Eqs. (18) by using the following quadrature formula [21]:

$$\begin{aligned} \int_{-1}^1 \Phi_k(\tau) K(\tau, \varphi) d\tau &= \sum_{m=1}^n a_m \psi_{km} \sum_{l=1}^n D_{lm} K(Z_l, \varphi), \\ D_{lm} &= -\frac{2}{n+1} \sin \frac{l\pi}{n+1} \sum_{p=1}^{n-1} \frac{\cos \frac{p(2m-1)\pi}{2n} \sin \frac{\pi lp}{n+1}}{p}, \\ Z_l &= \cos \frac{\pi l}{n+1}. \end{aligned}$$

Then we reduce the boundary conditions on the boundaries of the cross section of the cylinder to the following equations:

$$\begin{aligned}
& \sum_{k=1}^N A_k \left( \sum_{m=1}^n a_m \Psi_{km}^1 \sum_{l=1}^n D_{lm} G(Z_l, \varphi) + F_k^1(\varphi) \right) \\
& \quad + \sum_{k=1}^N B_k \left( \sum_{m=1}^n a_m \Psi_{km}^2 \sum_{l=1}^n D_{lm} G(Z_l, \varphi) + F_k^2(\varphi) \right) = P(\varphi), \\
& \sum_{k=1}^N A_k \left( \sum_{m=1}^n a_m \Psi_{km}^1 \sum_{l=1}^n D_{lm} E(Z_l, \varphi) + g_k(\varphi) \right) \\
& \quad + \sum_{k=1}^N B_k \left( \sum_{m=1}^n a_m \Psi_{km}^2 \sum_{l=1}^n D_{lm} E(Z_l, \varphi) + h_k(\varphi) \right) = 0.
\end{aligned} \tag{19}$$

By using collocation procedures at the nodes

$$\sigma_l = \frac{2\pi l}{N}, \quad l = 1, \dots, N,$$

and relations (19), we obtain the following system of linear equations for the coefficients  $A_k$  and  $B_k$

$$\begin{aligned}
& \sum_{k=1}^N A_k \left( \sum_{m=1}^n a_m \Psi_{km}^1 \sum_{l=1}^n D_{lm} G(Z_l, \sigma_l) + F_k^1(\sigma_l) \right) \\
& \quad + \sum_{k=1}^N B_k \left( \sum_{m=1}^n a_m \Psi_{km}^2 \sum_{l=1}^n D_{lm} G(Z_l, \sigma_l) + F_k^2(\sigma_l) \right) = P(\sigma_l), \\
& \sum_{k=1}^N A_k \left( \sum_{m=1}^n a_m \Psi_{km}^1 \sum_{l=1}^n D_{lm} E(Z_l, \sigma_l) + g_k(\sigma_l) \right) \\
& \quad + \sum_{k=1}^N B_k \left( \sum_{m=1}^n a_m \Psi_{km}^2 \sum_{l=1}^n D_{lm} E(Z_l, \sigma_l) + h_k(\sigma_l) \right) = 0.
\end{aligned} \tag{20}$$

The stress intensity factor (SIF)  $K^\pm$  at the opposite crack tips  $x_1 = \pm a$  are the quantities characterizing the behavior of stresses in the vicinity of the defect. In the analyzed case, they are given by the formulas

$$K^\pm = \sqrt{a} \lim_{\zeta \rightarrow \pm 1 \pm 0} \sqrt{\zeta^2 - 1} \tau_{y_1 z}(\alpha \tau, 0).$$

Solving the systems of equations (15), (20), we express the dimensionless values of these coefficients

$$k^\pm = \frac{K^\pm}{G\sqrt{a}}$$

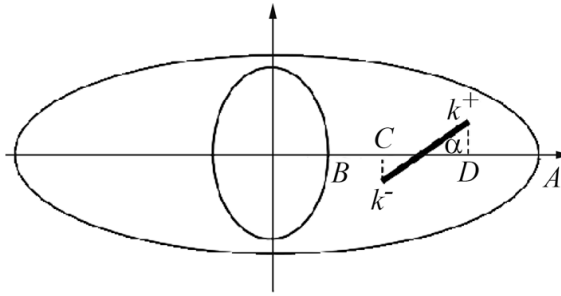


**Fig. 2.** Crack in a cylinder whose cross section is bounded by two ellipses.

by the following dependences:

$$k^+ = \frac{1}{2n} \left( \sum_{k=1}^N A_k \sum_{m=1}^n (-1)^m \psi_{km}^1 \cot \frac{\gamma_m}{2} + \sum_{k=1}^N B_k \sum_{m=1}^n (-1)^m \psi_{km}^2 \cot \frac{\gamma_m}{2} \right),$$

$$k^- = \frac{(-1)^{n+1}}{2n} \left( \sum_{k=1}^N A_k \sum_{m=1}^n (-1)^m \psi_{km}^1 \tan \frac{\gamma_m}{2} + \sum_{k=1}^N B_k \sum_{m=1}^n (-1)^m \psi_{km}^2 \tan \frac{\gamma_m}{2} \right),$$

where

$$\gamma_m = \frac{\pi(2m-1)}{2n}.$$

For the practical evaluation of the SIF, sufficiently accurate results were obtained by choosing the upper boundaries in approximation calculations as follows:  $N = n = 10$ .

### Numerical Analysis of the Intensity of Dynamic Stresses and Resonance Phenomena

For the numerical realization of the proposed method, we consider a cylinder whose cross section is bounded by two ellipses (Fig. 2) under a load  $P(\varphi) = \sin 2\varphi$  (the angle  $\varphi$  is measured from the point A on the major semi-axis of the outer contour). The eccentricities of the ellipses were assumed to be equal:  $\varepsilon = 0.5$ ; the ratio of the semi-axes of ellipses was specified as follows:  $r_1/r_0 = 0.5$ . The center of the crack was located on the major semi-axis of the external ellipse. The results of numerical investigations of the SIF within the frequency range and, in particular, their transition into the resonance mode in which the monotonicity of the frequency dependences of SIF is lost are presented in Fig. 3. In Fig. 3a, we show the results obtained for an inclined crack of constant length equal to one third of the distance between the vertices of the ellipses AB whose center is located at identical distances from the boundaries of the cross section. The analysis of the curves demonstrates that, prior to the attainment of the first resonance frequency, the SIF decrease as the inclination angle of the crack increases. The inclination angle also strongly affects the values of resonance frequencies. Thus, for the angles  $\alpha = 0^\circ$  and  $\alpha = 90^\circ$ , the resonance is absent. However, it is observed for the other inclination angles, where  $\kappa_0 \approx 2.6$ . Note that all analyzed cases are characterized by the resonance behavior of the SIF for  $\kappa_0 \approx 3.8$ .



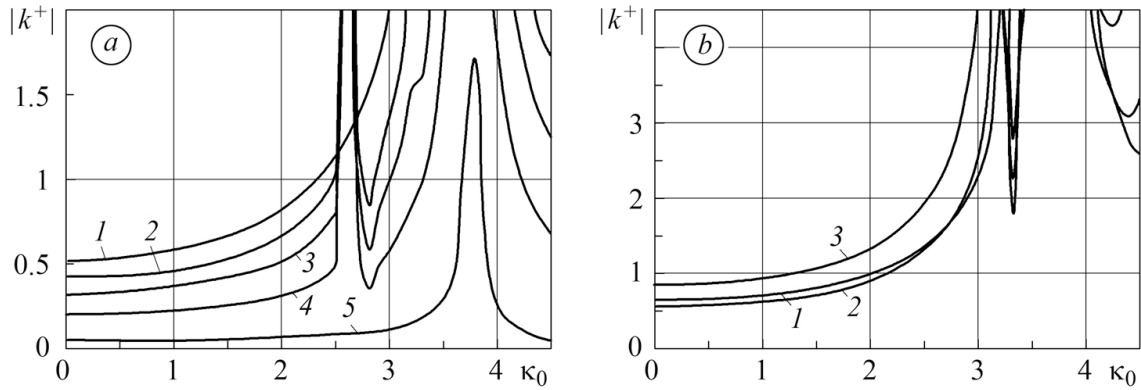


**Fig. 3.** Dependences of the absolute values of the SIF  $|k^+|$  on the dimensionless wave number  $\kappa_0 = \kappa_2 r_0$  for different angles of inclination of the crack [(a): (1)  $\alpha = 0^\circ$ ; (2)  $\alpha = 30^\circ$ ; (3)  $\alpha = 45^\circ$ ; (4)  $\alpha = 60^\circ$ ; (5)  $\alpha = 90^\circ$ ] and for  $\alpha = 0^\circ$  and different values of crack length [(b): (1)  $\gamma = 0.0946$ ; (2)  $\gamma = 0.1412$ ; (3)  $\gamma = 0.188$ ].

We also analyzed a crack oriented along the line AB with variable length (Fig. 3b). The left end of the crack  $C$  is fixed, while the right end  $D$  is made closer to the outer boundary of the cross section by varying the parameter  $\gamma = a/r_0$  from 0.0945 to 0.189 when the crack approaches the outer boundary. It was shown that this parametrization almost does not influence the value of the SIF  $k^-$  at the crack tip  $C$  remote from the outer contour. In the analyzed case, the SIF  $k^+$  at the opposite tip increases both with the crack length and as the crack approaches the outer boundary of the cross section. The resonance phenomena were observed within the frequency range  $3 < \kappa_0 < 4$ . The band of resonance frequencies is wider for the larger crack.

## CONCLUSIONS

The presence of a crack in an elastic hollow cylinder subjected to harmonic loading is accompanied by both the intense dynamic loads near the defect and their resonance behavior as a result of the generation of wave processes in the bounded domain. The analysis of antiplane deformation for which the vicinity of the crack is characterized by stress intensity factors of longitudinal shear proves to be especially convenient for the analysis of this kind. The determination of SIF in the frequency region is based on their relationship with the function of jump of the dynamic displacements on the crack and finding this function as a special solution of the integral equations on the crack with boundary conditions of dynamic loading of the cylindrical body on the lateral surfaces.

In the analyzed frequency range, we established the possibility of attainment of one or two resonances depending on the angle of inclination of the crack relative to the boundary of the body, unlike the case of a unique resonance in the same frequency range recorded in [22] for a cylinder with ribbon rigid inclusion. Both the variations of the inclination angle and the decrease in distance from the crack to the outer surface strongly affect the SIF and the rate of their passing into the resonance mode in the low-frequency region.

## REFERENCES

1. Z. T. Nazarchuk and V. R. Skal's'kyi, *Acoustic-Emission Diagnostics of Structural Elements*, Vol. 2: *Methodology of Acoustic-Emission Diagnostics* [in Russian], Nauka, Kiev (2009).
2. N. G. Stashchuk, *Problems of the Mechanics of Elastic Bodies with Cracklike Defects* [in Russian], Naukova Dumka, Kiev (1993).

3. V. G. Popov, "Comparison of displacement and stress fields in the process of diffraction of elastic shear waves on various defects: a crack and a thin rigid inclusion," *Dinam. Sist.*, Issue 2, 14–23 (1993).
4. D. D. Ang and L. Knopoff, "Diffraction of scalar elastic waves by a finite strip," *Proc. Math. Sci. USA*, **51**, No. 4, 593–598 (1964).
5. J. F. Loeber and G. C. Sih, "Diffraction of antiplane waves by a finite crack," *J. Acoust. Soc. Am.*, **44**, No. 1, 90–98 (1968).
6. G. Zi, H. Chen, J. Xu, and T. Belytchko, "The extended finite element method for dynamic fractures," *Shock Vibrat.*, **12**, No. 1, 9–23 (2005).
7. A. K. Mal, "Interaction of elastic waves with a Griffith crack," *Int. J. Eng. Sci.*, **8**, No. 9, 763–766 (1970).
8. V. V. Mykhas'kiv and O. I. Stepanyuk, "Boundary integral analysis of the symmetric dynamic problem for an infinite bimaterial solid with an embedded crack," *Meccanica*, **36**, No. 4, 479–495 (2001).
9. V. Mykhas'kiv, "Transient response of a plane rigid inclusion to an incident wave in an elastic solid," *Wave Motion*, **41**, No. 2, 133–144 (2005).
10. V. Mykhas'kiv, I. Zhadynskyi, and C. Zhang, "Elastodynamic analysis of multiple crack problem in 3D bimetals by a BEM," *Int. J. Num. Meth. Biomed. Eng.*, **26**, No. 12, 1934–1946 (2010).
11. V. G. Popov, "Harmonic vibrations of a half space with a surface-breaking crack under conditions of out-of-plane deformation," *Izv. Ross. Akad. Nauk, Mekh. Tverd. Tela*, No. 2, 96–105 (2013); **English translation: Mech. Solids**, **48**, No. 2, 194–202 (2013).
12. V. G. Popov, "Interaction between elastic longitudinal shear waves and radially located cracks," *Prikl. Mekh.*, **34**, No. 2, 60–66 (1998).
13. I. Nistor, O. Pantale, and S. Caperaa, "Numerical implementation of the extended finite-element method for dynamic crack analysis," *Adv. Eng. Software*, **39**, No. 7, 573–587 (2008).
14. P. Hosseini-Tehrani, A. R. Hosseini-Godarzi, and M. Tavangar, "Boundary element analysis of stress intensity factor  $K_I$  in some two-dimensional dynamic thermoelastic problems," *Eng. Anal. Bound. Elem.*, **29**, No. 3, 232–240 (2005).
15. F. Chirino and J. Domingues, "Dynamic analysis of cracks using boundary element method," *Eng. Fract. Mech.*, **34**, No. 5-6, 1051–1061 (1989).
16. A. A. Bobylev and Yu. A. Dobrova, "Application of the boundary-element method to the evaluation of forced vibration of elastic bodies of finite sizes with cracks," *Vest. Kharkiv. Nats. Univ. Mat. Model. Inform. Tekhnol. Avtom. Sist. Upravl.*, No. 590, 49–54 (2003).
17. C. Zhang, "A 2D hypersingular time-domain traction BEM for transient elastodynamic crack analysis," *Wave Motion*, **35**, No. 1, 17–40 (2002).
18. V. B. Poruchikov, *Methods of the Dynamic Theory of Elasticity* [in Russian], Nauka, Moscow (1986).
19. I. N. Vekua, *New Methods for the Solution of Elliptic Equations* [in Russian], OGIZ, Moscow (1948).
20. S. M. Belotserkovskii and I. K. Lifanov, *Numerical Methods in Singular Integral Equations* [in Russian], Nauka, Moscow (1985).
21. V. I. Krylov, *Approximate Calculation of the Integrals* [in Russian], Nauka, Moscow (1967).
22. O. I. Kirilova, "Harmonic vibrations of longitudinal shear of an infinite cylinder of arbitrary cross section with a system of inclusions," *Izv. Nats. Akad. Nauk Arm. Mekhanika*, **65**, No. 4, 26–32 (2012).